24th COBEM - 2017

24th ABCM International Congress of Mechanical Engineering
December 3-8, 2017, Curitiba, PR, Brazil

COBEM-2017-1698
Growth of even and odd instability modes in compressible binary jet flows

J. K. Rogenski
L. F. de Souza
Departamento de Matemática Aplicada e Estatística, Instituto de Ciências Matemáticas e de Computação, Universidade de São Paulo
josuelkr@gmail.com, lefraso@icmc.usp.br

M. T. de Mendonça
Instituto de Aeronáutica e Espaço, Departamento de Ciências e Tecnologia Aeroespacial, Ministério da Defesa
marcio_tm@yahoo.com

P. J. Morris
Aerospace Engineering, College of Engineering, The Pennsylvania State University
pjm@psu.edu

Abstract. *The mixing process between different gas species is particularly important in combustion and on the design of jet engines composed by a bypass flow and a core stream. When connecting the efficiency of a mixture process to turbulence, stability of the given baseflow becomes an important way to understand the physics of these problems. Transition of base flow profile composed by a planar jet of an A-specie immersed in a B-specie co-flow is studied. Stability of these compressible, binary and planar jets is carried out by means of direct numerical simulations. Both the sinuous and varicose modes show to be potentially unstable. The most dangerous mode is the sinuous one for the cases under consideration. Nonlinear topological characteristics are captured and discussed in terms of velocity and vorticity distributions.*

Keywords: *laminar-turbulent transition, Direct Numerical Simulation, compressible jets, binary mixture*

1. INTRODUCTION

Combustion systems efficiency is highly connected with the mixture between fuel and oxidizer. The study of the stability of the system in such cases presents valuable information about the process. Based on these information, one may control temperature distribution and reduce both noise and pollutant emissions. Stability and acoustics of compressible coaxial jets were investigated by Gloor *et al.* (2013) and the relevant parameters on the development of acoustic and hydrodynamic modes were identified considering the solution of the Rayleigh equation. Here we consider the same problem by direct numerical simulation, but for a mixture of different gases and by obtaining the base flow solution through the solution of the Navier-Stokes equations for the binary system, similarly to Dahl and Morris (1997a,b) and Mendonca (2014). We seek agreement with results provided by Mendonca (2014), which demonstrates base flow profiles obtained through boundary layer theory are different from the classical profiles based on hyperbolic secant and tangent functions.

2. FORMULATION AND NUMERICAL METHOD

The compressible and inviscid Euler system of equations is adopted to represent the evolution of compressible, binary and planar jet profiles. Both base flow and disturbances are considered two-dimensional. The vector of conserved variables $\mathbf{q}$ is composed by the density ρ, the velocity vector components u and v, the pressure p, the energy e and the mass fraction s_1 of the reference specie.

The system of equations is

$$\frac{\partial \mathbf{q}}{\partial t} + \frac{\partial \mathbf{f}}{\partial x} + \frac{\partial \mathbf{g}}{\partial y} = 0, \tag{1}$$

where $\mathbf{f}$ and $\mathbf{g}$ are the flux vectors (Lacerda, 2016). Here, we emphasize the equation for s_1 which is given by

$$\frac{\partial \rho s_1}{\partial t} + \frac{\partial \rho u s_1}{\partial x} + \frac{\partial \rho v s_1}{\partial y} = \frac{1}{Re}\frac{1}{Pr}\frac{1}{Le}\left[\frac{\partial}{\partial x}\left(D_{12}\rho\frac{\partial s_1}{\partial x}\right) + \frac{\partial}{\partial y}\left(D_{12}\rho\frac{\partial s_1}{\partial y}\right)\right] \tag{2}$$

where Re, Pr and Le are respectively the Reynolds, Prandtl and Lewis dimensionless numbers.

2.1 The mixture properties

Mixture quantities are functions of both species concentration and temperature. The equation of state

$$1 = \rho R_u T \left(s_1 X_1 + s_2 X_2\right) \tag{3}$$

is adopted to calculate the density as a function of the temperature of the mixture T and mass fractions s_1 and s_2. The universal gas constant is represented by R_u. Considering the subscript *'ratio'* as the quotient between inner and outer jet properties, the gas constant and the specific heat at a constant pressure are

$$R = s_1 + R_{\text{ratio}}(1 - s_1) \text{ and } c_p = s_1 + c_{p_{\text{ratio}}}(1 - s_1). \tag{4}$$

The dynamic viscosity of the mixture μ is

$$\mu = \frac{X_1 \mu_1}{X_1 + X_2 \phi_{12}} + \frac{X_2 \mu_2}{X_2 + X_1 \phi_{21}}, \tag{5}$$

assuming

$$\phi_{12} = \frac{\left[1 + \left(\mu_1/\mu_2\right)^{1/2} \left(\mathcal{M}_2/\mathcal{M}_1\right)^{1/4}\right]^2}{\left[8\left(1 + \mathcal{M}_1/\mathcal{M}_2\right)\right]^{1/2}}, \qquad \phi_{21} = \phi_{12} \frac{\mu_1}{\mu_2} \frac{\mathcal{M}_1}{\mathcal{M}_2}, \tag{6}$$

where $\mathcal{M}_i$ and X_i are the molar mass and the molar fraction of the i-species.

The thermal conductivity of the mixture λ is calculated as

$$\lambda = \frac{X_1 \lambda_1}{X_1 + X_2 \phi_{12}} + \frac{X_2 \lambda_2}{X_2 + X_1 \phi_{21}}, \tag{7}$$

considering

$$\phi_{12} = \frac{\left[1 + \left(\lambda_1/\lambda_2\right)^{1/2} \left(\mathcal{M}_2/\mathcal{M}_1\right)^{1/4}\right]^2}{\left[8\left(1 + \mathcal{M}_1/\mathcal{M}_2\right)\right]^{1/2}} \text{ and } \phi_{21} = \phi_{12} \frac{\lambda_1}{\lambda_2} \frac{\mathcal{M}_1}{\mathcal{M}_2}. \tag{8}$$

2.2 The base flow profile

The inlet streamwise velocity distribution of the adopted base flow profile is

$$u_b(x_0, y) = (1 - cf) u_1, \tag{9}$$

where cf is a non-negative constant. The function u_1 is

$$u_1 = \frac{1 + f}{2},$$

where

$$f = \tanh\left[\frac{3}{8}\left(\frac{R}{y} - \frac{y}{R}\right)\right].$$

It is also considered $v_b(x_0, y) = 0$ and $T_b(x_0, y) = 1$. The mass fraction of the reference gas is $s_1(x_0, y) = 0.85 u_1 + 0.1$.

2.3 The numerical method

Solutions are obtained numerically through direct numerical simulation. High-order compact finite difference schemes are adopted to approximate spatial derivatives. Temporal evolution is done considering a $4th-$ order Runge-Kutta method (Lele, 1992; Souza *et al.*, 2005; Petri *et al.*, 2015).

In general, following Lacerda (2016) and Mendonca (2014), the numerical procedure is summarized by the following algorithm:

(a) specify initial conditions for u, v, s_1 and T in all numerical domain;

(b) calculate ρ considering

$$\rho = \left[s_1\, T + (1 - s_1)\, T\, R_{\text{ratio}}\right]^{-1}. \tag{10}$$

(c) at each step of the Runge-Kutta method calculate

(c.1.) the mass fraction of the mixture

$$m = \left(s_1 + \frac{1 - s_1}{m_{\text{ratio}}} \right)^{-1}, \tag{11}$$

where m_{ratio} is the mass ratio between specie 2 and specie 1.

(c.2.) molar fraction of the mixture

$$\chi_1 = s_1 \, m \tag{12}$$

and

$$\chi_2 = \frac{s_2 \, m}{m_{\text{ratio}}}. \tag{13}$$

(c.3.) the dynamic viscosity of both species, obtained by the use of the potential law.

(c.4.) the viscosity of the mixture

$$\mu = \frac{\chi_1 \mu_1}{\chi_1 + \chi_2 \phi_{12}} + \frac{\chi_2 \mu_2}{\chi_2 + \chi_1 \phi_{21}}, \tag{14}$$

where $\phi_{12} = \dfrac{\left(1 + \sqrt{\frac{\mu_1}{\mu_2}} m_{\text{ratio}}^{\frac{1}{4}}\right)^2}{\sqrt{8\left(1 + \frac{1}{m_{\text{ratio}}}\right)}}$ and $\phi_{21} = \phi_{12} \frac{\mu_1}{\mu_2} \frac{1}{m_{\text{ratio}}}$.

(c.5) the potential law is also used to calculate the thermal conductivity of each specie.

(c.6) the thermal conductivity of the mixture

$$k = \frac{\chi_1 k_1}{\chi_1 + \chi_2 \phi_{12}} + \frac{\chi_2 k_2}{\chi_2 + \chi_1 \phi_{21}}, \tag{15}$$

where $\phi_{12} = \dfrac{\left(1 + \sqrt{\frac{k_1}{k_2}} m_{\text{ratio}}^{\frac{1}{4}}\right)^2}{\sqrt{8\left(1 + \frac{1}{m_{\text{ratio}}}\right)}}$ and $\phi_{21} = \phi_{12} \frac{k_1}{k_2} \frac{1}{m_{\text{ratio}}}$.

(c.7.) the right-hand side of the system.

(d) update boundary conditions based on Lacerda (2016).

(e) a high order numerical filter (Lele, 1992) is applied in both directions.

Initial disturbances in a base flow profile are here considered as inflow boundary conditions represented by a set of eigenfunctions generated by linear stability theory results (Mendonca, 2014). Buffer zones are applied in both the far field and outflow boundaries.

Computational efficiency is achieved by the use of a parallel domain decomposition technique in both directions.

3. RESULTS AND DISCUSSION

Adopted physical values are considered assuming 300 K temperature and 1 atm pressure. Quantities are made dimensionless considering reference values provided by Tab. 1

Amplification rates $-\alpha_i$ and wavenumbers ω of both the sinuous and varicose modes of binary jet flows represented by $O_2 - H_2 - O_2$ and $H_2 - O_2 - H_2$ binary jet flows are presented in Fig. 1. These curves are obtained by solving the associated linear stability theory problem. Here, linear stability results are important in two ways: to provide sets of eigenfunctions used as inflow conditions and to provide information about the most dangerous wavenumber of each case.

By Fig. 1, one may observe both sinuous and varicose modes are potentially unstable. The sinuous mode proved to be more unstable than the varicose one. The most dangerous case is the sinuous mode represented by $H_2 - O_2 - H_2$.

Table 1: Gas properties at $300K$ and 1 atm

	H_2	O_2
$\mathcal{M}$ [g mol^{-1}]	2.02	32
R [J kg^{-1} K^{-1}]	4124.5	259.8
c_p [J kg^{-1} K^{-1}]	14310.9	918.4
c_v [J kg^{-1} K^{-1}]	10160	659
μ [kg m^{-1} s^{-1}]	8.9738e-6	2.0743e-5
k [W m^{-1} K^{-1}]	0.0266	0.1878
ρ [kg m^{-3}]	1.2998	0.08189
D_{12} [m^2 s^{-1}]	7.8842e-5	7.8842e-5
γ	1.405	1.395
Pr	0.7081	0.7069
Le	2.020	0.304

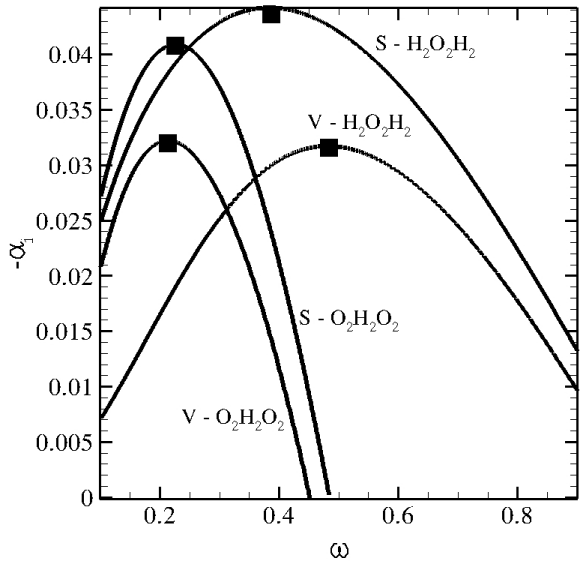

Figure 1: Linear stability theory results for two gas mixture configurations. In both plots, spatial amplification rates are given as a function of frequency

3.1 Nonlinear evolution of the vortices

Nonlinear simulations consider Reynolds number $Re = 1 \times 10^3$ and Mach number $Ma = 1.25$. In Fig. 2, a temporal Fourier analysis is presented for the evolution of the sinuous mode in a $O_2 - H_2 - O_2$ binary jet and $\omega = 0.2286$. This specific frequency represents the maximum amplification for the $O_2 - H_2 - O_2$ case according to the linear stability results.

Well defined regions of receptivity, linear growth, non-linear growth and buffer zone can be observed.

The sinuous nature of the instability is observed in Fig. 3. Both vorticity and mass fraction isocontourns of the flow are presented. Vortical structures develop and become more complex downstream. It is also possible to observe the effect of jet spreading.

Instability can also be observed for the $H_2 - O_2 - H_2$ case – see Fig. 4. For this case, $\omega = 0.386$ represents the maximum amplification rate according to the linear stability theory. However, the nature of vortices are quite different from the previous case. Effects of jet spreading are less pronounced. Vortical structures seems to be confined near the jet region due to both velocity and molar mass of the inner specie be higher than the outer one.

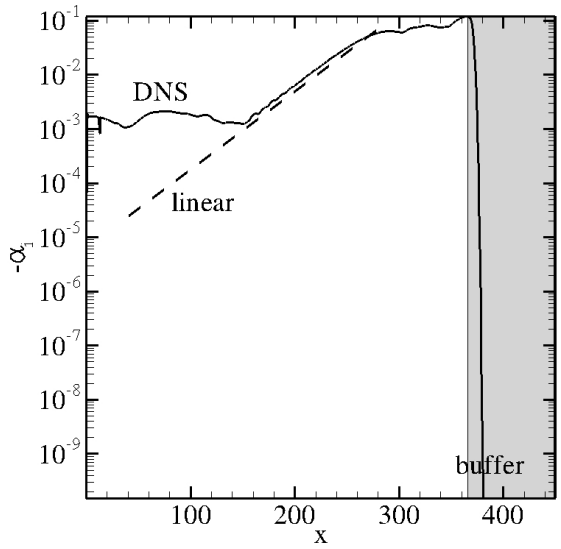

Figure 2: Fourier analysis of the sinuous mode. Stability of $O_2 - H_2 - O_2$ binary jet with $\omega = 0.2286$

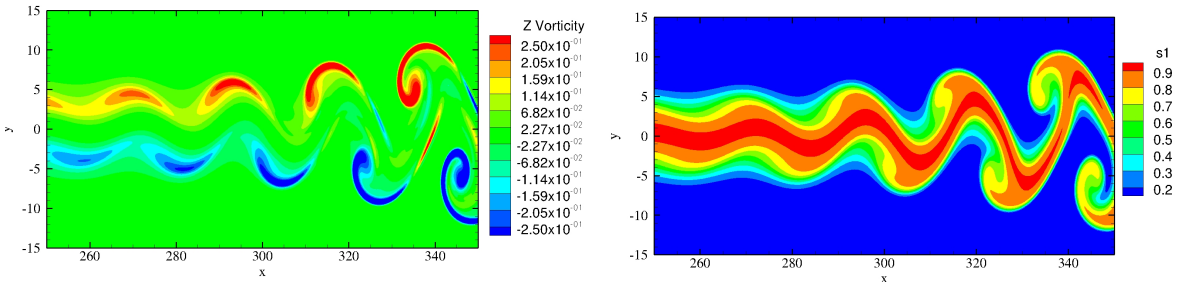

(a) ω (b) s_1

Figure 3: Vorticity and mass fraction distributions of the $O_2 - H_2 - O_2$ binary jet in the nonlinear region – Sinuous mode

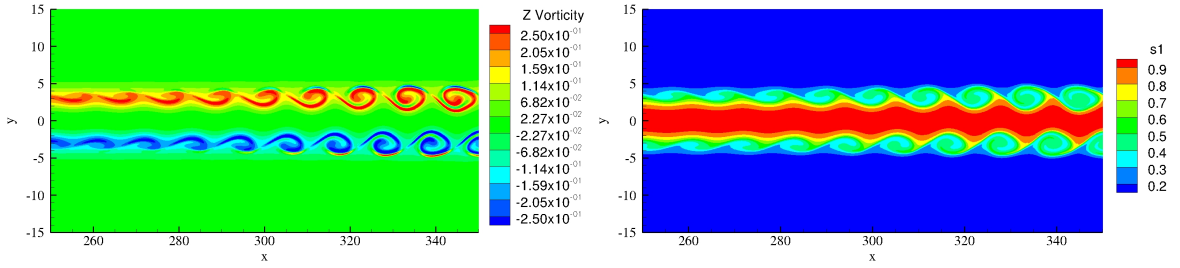

(a) ω (b) s_1

Figure 4: Vorticity and mass fraction distributions of the $H_2 - O_2 - H_2$ binary jet in the nonlinear region – Sinuous mode

4. CONCLUSIONS

Transition studies on binary compressible jet flows are conducted by means of numerical simulations. Both sinuous and varicose modes provide to be potentially unstable. The sinuous mode shows to be the most dangerous mode and may dominate transition. Topological aspects of the vortical structures are qualitatively different and depend on the ratio between inner and outer gas species properties.

5. ACKNOWLEDGEMENTS

Authors acknowledge financial support provided by CNPq project #401032/2014-0 and Fapesp.

6. REFERENCES

Dahl, M.D. and Morris, P.J., 1997a. "Noise from supersonic coaxial jets, part 1: Mean flow predictions". *Journal of Sound and Vibration*, Vol. 200, No. 5, pp. 643–663.

Dahl, M.D. and Morris, P.J., 1997b. "Noise from supersonic coaxial jets, part 2: Normal velocity profile". *Journal of Sound and Vibration*, Vol. 200, No. 5, pp. 665–699.

Gloor, M., Obrist, D. and Kleiser, L., 2013. "Linear stability and acoustic characteristics of compressible, viscous, subsonic coaxial jet flow". *Physics of Fluids*, Vol. **25**, pp. 084102–1–084102–25.

Lacerda, J.F., 2016. *Aeroacustica computacional atraves de Simulacao Numerica Direta*. Ph.D. thesis, Universidade de São Paulo.

Lele, S., 1992. "Compact finite difference schemes with spectral-like resolution". *Journal of Computational Physics*, Vol. 103, pp. 16–42.

Mendonca, M.T., 2014. "Linear stability analysis of binary compressible mixing layers modified by a jet or a wake deficit". In *52nd AIAA Aerospace Sciences Meeting and Exhibit*. National Harbor, Maryland, pp. 1–13.

Petri, L.A., Sartori, P., Rogenski, J.K. and de Souza, L.F., 2015. "Verification and validation of a direct numerical simulation code". *Computer Methods in Applied Mechanics and Engineering*, Vol. 291, pp. 266–279.

Souza, L.F., Mendonça, M.T. and Medeiros, M.A.F., 2005. "The advantages of using high-order finite differences schemes in laminar turbulent transition studies". *International Journal for Numerical Methods in Fluids*, Vol. 48, pp. 565–592.

7. RESPONSIBILITY NOTICE

The authors are the only responsible for the printed material included in this paper.